FISSION NEUTRON MULTIPLICITY CALCULATIONS

H. Märten, A. Ruben, and D. Seeliger
Technische Universität Dresden, Institut für Kern- und Atomphysik
Mommsenstrasse 13, D-O-8027 Dresden, Germany

Abstract: *A model for calculating neutron multiplicities in nuclear fission is presented. It is based on the solution of the energy partition problem as function of mass asymmetry within an phenomenological approach including temperature-dependent microscopic energies. Nuclear structure effects on fragment de-excitation, which influence neutron multiplicities, are discussed. Temperature effects on microscopic energy play an important role in induced fission reactions. Calculated results are presented for various fission reactions induced by neutrons. Data cover the incident energy range* 0-20 *MeV, i.e. multiple chance fission is considered.*

1. INTRODUCTION

Fission neutron multiplicity data for major as well as minor actinides are of essential importance in various nuclear technology applications. Together with the availability of experimental results, consistent theoretical approaches are necessary preconditions for further evaluations. The consideration of the energy balance equation

$$\bar{Q} + E^*_{cn} = \overline{TKE} + \bar{E}^*_{tot}, \qquad (1)$$

where Q - total energy release in the fission process,
E^*_{cn} - excitation energy of the fissioning nucleus,
TKE - total kinetic energy of the fragments,
$\bar{E}^*_{tot}$ - total excitation energy of the fragments,
must be required obviously. The average number of fission neutrons is strongly correlated with $\bar{E}^*_{tot}$. However, the reliable calculation of this quantity can only be performed considering the complexity of the fission process in an adequate manner and accounting for fragment de-excitation due to neutron and γ-ray emission mainly. The present work relies on a simple scission point model /1/ for solving the energy partition problem in fission, i.e. the partition of E^*_{tot} on both complementary fragments, as function of mass asymmetry. In addition to previous descriptions, systematic trends of various energy terms with

relevance to scission point conditions as well as nuclear structure effects in fragment de-excitation are discussed in more detail.

2. ENERGY PARTITION MODEL (SCISSION POINT MODEL)

2.1. Energy balance equation

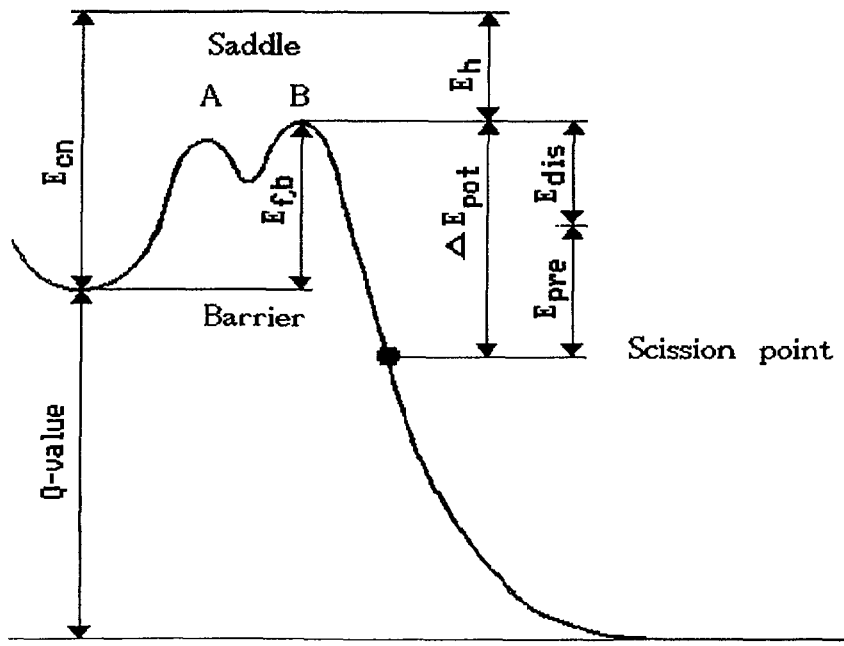

Fig. 1 Scheme of induced nuclear fission illustrating various energy terms explained in the text

The basic idea of the scission point model /1/ used is a detailed energy balance for any induced or spontaneous fission reaction. Fig. 1 represents a general scheme of fission illustrating the energy terms which are important during the fission process starting with a compound-nucleus with excitation energy E_{cn}, passing the double-humped fission barrier with the heights $E_{f,A}$ and $E_{f,B}$, and arriving at the scission point. The scission point energy terms are defined with reference to saddle B. Here, the intrinsic excitation energy is assumed to be

$$E_h = E_{cn} - E_{f,B} - \Delta_p \qquad (2)$$

with the constraint $E_h \geq 0$, i.e. E_h vanishes in the case of spontaneous and sub-barrier fission. Δ_p is the pairing gap above barrier B including a temperature dependence according to Kristiak /2/.

The potential energy release between second saddle and scission is assumed to be the sum of pre-scission kinetic energy E_{pre} and dissipative energy E_{dis}. The sum $E_{dis}+E_h$ corresponds to the total intrinsic energy at scission point (E_{int}) and is distributed on the complementary fragments according to statistical assumptions. The energy balance equation in more detailed form reads

$$\bar{Q}\left[\frac{A_1}{A_2}\right] + E_{cn} = \underbrace{E_{pre} + E_{coul}\left[\frac{A_1}{A_2}\right]}_{\overline{TKE}\left[\frac{A_1}{A_2}\right]} + \underbrace{E_{def}^{(1)} + E_{def}^{(2)} + E_{dis} + E_h}_{\bar{E}^*\left[\frac{A_1}{A_2}\right]} \qquad (3)$$

$$F\left[\frac{A_1}{A_2}\right] \qquad E_{int}^{(1)}+E_{int}^{(2)}$$

where

E_{coul} - Coulomb potential energy at scission,

$E_{def}^{(i)}$ - deformation energy of fragment (i) at scission,

E_{dis} - dissipative energy,

$E_{int}^{(i)}$ - intrinsic excitation of fragment (i) at scission,

E_h - intrinsic excitation energy ("heat") at second saddle,

F - potential energy at scission for given mass asymmetry,

E_{pre} - pre-scission kinetic energy.

The deformation-dependent part of scission point potential F is minimized in order to deduce the most probable energy partition at scission.

For neutron multiplicity calculations, the "asymptotic" excitation energy of a single fragment (after dissipation of deformation energy into intrinsic energy, but before de-excitation) is of special interest. It is obtained by

$$\bar{E}^*(A_i) = E_{def}^{(i)} + E_{dis}^{(i)} \qquad i=1,2\ . \qquad (4)$$

Further, the total kinetic energy of fission fragments for given mass number ratio is given by

$$\overline{TKE}(A_1/A_2) = E_{coul}(A_1/A_2) + E_{pre}. \qquad (5)$$

2.2. Liquid drop model and microscopic energies

Within the present scission point model TSM (two-spheroid model /1/), the scission configuration is assumed to consist of two spheroidally shaped fragments, whose dips are separated by a distance d ~ 1 fm (consequence of nuclear interaction of both fragments with diffuse surface). E_{coul} is assumed to be the coulomb repulsion energy of two charges effectively located at the centers of the fragments. The deformation energy is taken to be quadratic in radius change with reference to a spherical nucleus with radius $R^{(i)}$ considering the fragment deformability α. As shown by Terrell /3/, the deformability α is related to the stiffness parameter (quadruple deformation).

Minimizing the potential energy F at scission in regard to variation of fragment deformation, the most probable scission configuration is determined. However, nuclear stiffness influences the amount of deformation energy for given deformation essentially. Using an empirical relation between stiffness and shell correction energy $\delta W(A)$ /4/, the TSM has been used to deduce effective $\delta W(A)$ for typical deformed fragments at scission. Hence, the remarkable deficiencies of the simple TSM are compensated by deducing the microscopic energy from well-known fission data. However, the diminution of shell correction energy due to intrinsic temperature τ at scission has to be considered.The temperature τ can be calculated on the basis of the Fermi-gas model approach,

$$E^{(i)}_{int}(A) = a^{(i)}(A)\, \tau^2 \qquad (6)$$

($a^{(i)}(A)$ - level density parameter according to Ignatyuk et al. /5/). The intrinsic energy at scission E_{int} includes both dissipative energy E_{dis} and heat energy above the second fission barrier E_h. The partition on the fragments is defined by the condition of equal intrinsic temperatures τ of complementary fragments at scission ($\tau^{(1)}=\tau^{(2)}$).

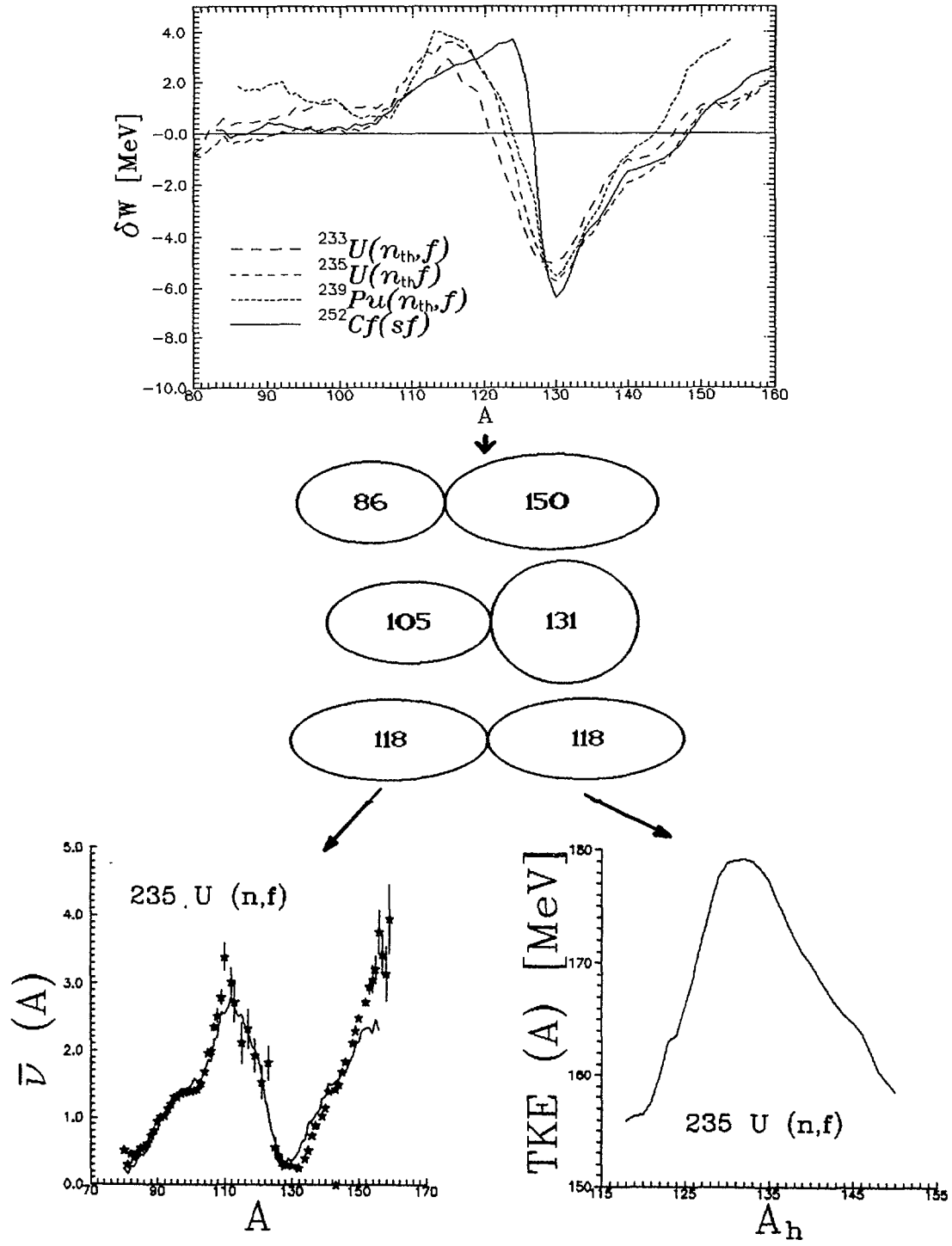

Fig. 2 Calculated semi-empirical shell correction energies (τ=0) for different fission reactions. The influence of shell structure on the fragment characteristics is illustrated for three fragment pairs with different deformations. Thus, the connection between high deformation and high neutron emission /6/ (left) as well as between vanishing deformation and maximum TKE /7/ (right) is illustrated.

For applications of the formalism outlined above to any fission reaction, sets of semi-empirical, model-dependent shell-correction energies were deduced for the well-investigated fission reactions $^{252}Cf(sf)$ and $^{235}U(n_{th},f)$. Both sets are nearly identical /1/ and correspond to microscopic calculations qualitatively. The actual $\delta W(A)$ function are determined by interpolation of the parameter set (reduced to zero temperature) and by considering the intrinsic excitation. Fig. 2 shows the calculated phenomenological shell correction energies reduced to zero excitation at scission ($\tau=0$) for different fission reactions. It has been found that the dependence $\delta W(A)$ /1/ is quite similar for fissioning systems (Th-Cf) in the most probable mass regions. On the other hand, a direct correspondence between fragment characteristics and deformation is obvious.

2.3. Dissipative energy

A relatively crucial problem in nuclear fission studies is the degree of intrinsic excitation during the descent from second saddle point to scission point.One method to deduce E_{dis} by analyzing the proton pairing effect δ_p was presented by Gönnenwein /8/. Dissipative energies, which increase with fissility Z^2/A from about 3 MeV in the case of Th up to 11 MeV for Cf, were estimated.

First applications of the TSM have shown that the calculated energy partitions are rather sensitive to the dissipative energy. It has been found that an approximative parameterization of Gönnenwein's E_{dis} data for any TSM application is not reliable. Therefore, dissipative energies have been adjusted for many fissioning systems in the Th-Cf region as described in /1/, i.e. that the TSM set of equations is solved by including experimental TKE und $\bar{\nu}$ data. Note that in contrast to /1/ the proton pairing for ^{252}Cf is assumed to be about 5%. This yields a higher dissipative energy for heavy fissioning nuclei as deduced in /1/. These new values as well as the data deduced by Gönnenwein are plotted in Fig. 3 for different fission reactions.

2.4. Pre-scission kinetic energy

E_{pre} can be understood as the translational part of collective degrees of freedom with relevance to the descent from saddle point to scission point. For TSM calculations, E_{pre} as

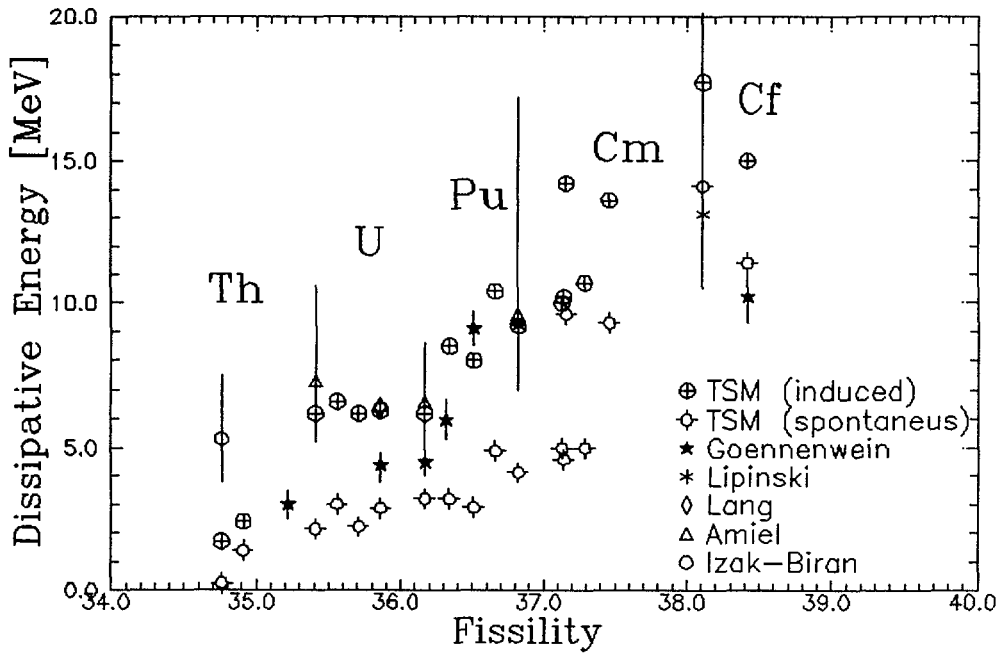

Fig. 3 TSM fitted dissipative energies as function of fissility Z^2/A for different fission reactions in comparison with the data deduced from proton odd-even effects /9-12/ by Gonnenwein /8/ (guide line for induced fission)

function of mass and charge of the fissioning nucleus was approximated on the basis of /8/ by

$$E_{pre} = \left[2.24 \frac{Z_{FN}^2}{A_{FN}} - 69.5 \right] \text{MeV}, \qquad (7)$$

2.5. Spontaneous versus threshold fission

Obviously, the starting conditions for spontaneous and threshold fission are quite different. In the latter case, ΔE_{pot} is effectively enhanced (with reference to spontaneous fission) by the value of the fission barrier. To deduce the consequence to differences in E_{dis} and E_{pre}, we assume that the fragmentation process is separable into two phases /1/:

(i) *Charge separation connected with rather strong friction:* The main part of potential energy gain is concentrated on E_{dis}.

(ii) *Neck formation and rupture in conjunction with a pre-acceleration of the nascent fragments:* The potential energy release in this phase yields higher E_{pre} mainly.

It is likely that differences between threshold and spontaneous (tunneling) fission concern the first phase predominantly. Consequently, for sufficiently high ΔE_{pot},

especially the dissipative energy should differ for spontaneous and threshold fission. E_{pre} can be assumed to be equal in both cases. As shown in Fig. 4 (right), $\overline{TKE}$ differences are very small for $Z^2/A \geq 36$, . On the other hand, there are increasing differences in the average neutron multiplicity $\Delta\bar{\nu}$ as a measure of dissipative energy (Fig. 4, left).

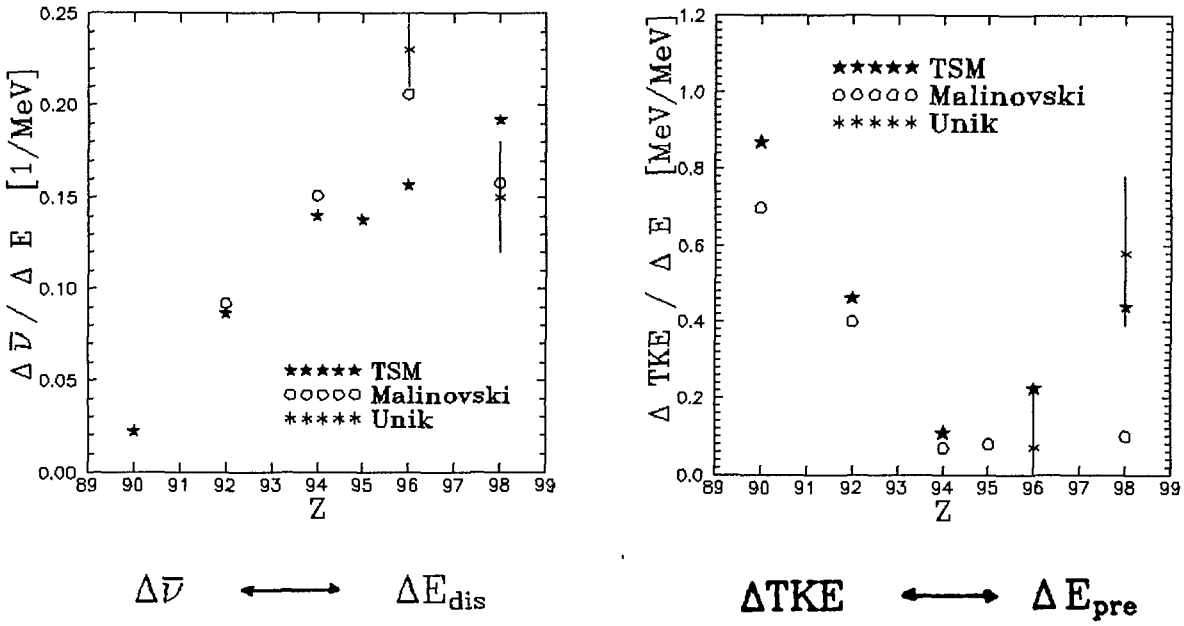

$\Delta\bar{\nu} \longleftrightarrow \Delta E_{dis}$ $\qquad$ $\Delta TKE \longleftrightarrow \Delta E_{pre}$

Fig. 4 Changes of $\bar{\nu}$ and TKE from spontaneous to threshold fission according to Malinovski /13/ and Unik /14/ and fitted results obtained in the framework of TSM

However, for rather light fissioning nuclei ($Z^2/A \leq 36$), phase (2) is shifted close to barrier penetration in the case of spontaneous fission. E_{pre} and, consequently, $\overline{TKE}$ becomes lower compared to threshold fission. In this case smaller differences in E_{dis} yield in a decrease of $\Delta\bar{\nu}$. As depicted in Fig. 4 this interpretation is confirmed by the experimental-data trends.

3. FRAGMENT DE-EXCITATION

To deduce fission fragments neutron multiplicities an energy balance of fragment de-excitation was proposed /1/ including the evaporation of neutrons (multiplicity $\bar{\nu}$, average energy $\bar{\varepsilon}$ in the center-of-mass system CMS) and γ-ray emission (average total energy $\bar{E}_\gamma$),

$$\bar{E}^*(A_i) = \bar{\nu}(A_i)\,(\bar{B}_n(A_i) + \bar{\varepsilon}(A_i)) + \bar{E}_\gamma(A_i). \qquad (8)$$

The average neutron separation energy for primary fragments $\bar{B}_{n,o}(A)$, i.e. before neutron emission, is calculated on the basis of mass tables /15/ using an approximative charge distribution according to Wahl /16/. To consider the increase of $\bar{B}_n(A)$ with $\bar{\nu}$ due to the shift of the fission fragments towards the line of β-stability, these data are corrected according to

$$\bar{B}_n(A) = \bar{B}_{n,o}(A) + C\ \bar{\nu}(A) \qquad (9)$$

with the correction factor C ($\approx$ 0.2 for U, $\approx$ 0.1 for Cf). Fig. 5 shows the increase of the neutron separation energy with neutron emission as function of fragment mass for three fission reactions. The different lines correspond to those values of the emission of the first, second and third neutron.

According to the results of Frehaut /17/, the average total gamma energy is assumed to be linear in neutron multiplicity. Thus, $\bar{E}_\gamma(A_i)$ is given in the Th-Cf region by the following approximation

$$\bar{E}_\gamma(A) = [\ G_1(A)\ \bar{\nu}(A) + 2.2\ ]\ \text{MeV}\ , \qquad (10)$$

where G_1 is a parameter depending on A /17/.

4. NEUTRON MULTIPLICITY VERSUS FRAGMENT MASS NUMBER AND TOTAL KINETIC ENERGY

The dependence of neutron multiplicity versus fragment mass number and total kinetic energy has been studied in several experiments /18-20/ in the case of ^{252}Cf(sf). It has been found a nearly linear decrease of $\bar{\nu}$(TKE,A) with TKE for fixed A in a wide TKE and A range which can be understood in first order on the basis of energy conservation (eq. (1)). However, shell-effects depending on deformation and temperature at scission influence the slope $\partial\bar{\nu}/\partial$TKE for individual fragments.

Applying the TSM /21/ to solve this energy partition problem for fixed TKE (constraint) it was possible to reproduce the linear dependence. As shown in Fig. 6, the calculated slopes $\partial\bar{\nu}/\partial$TKE as function of fragment mass number are in a good agreement with

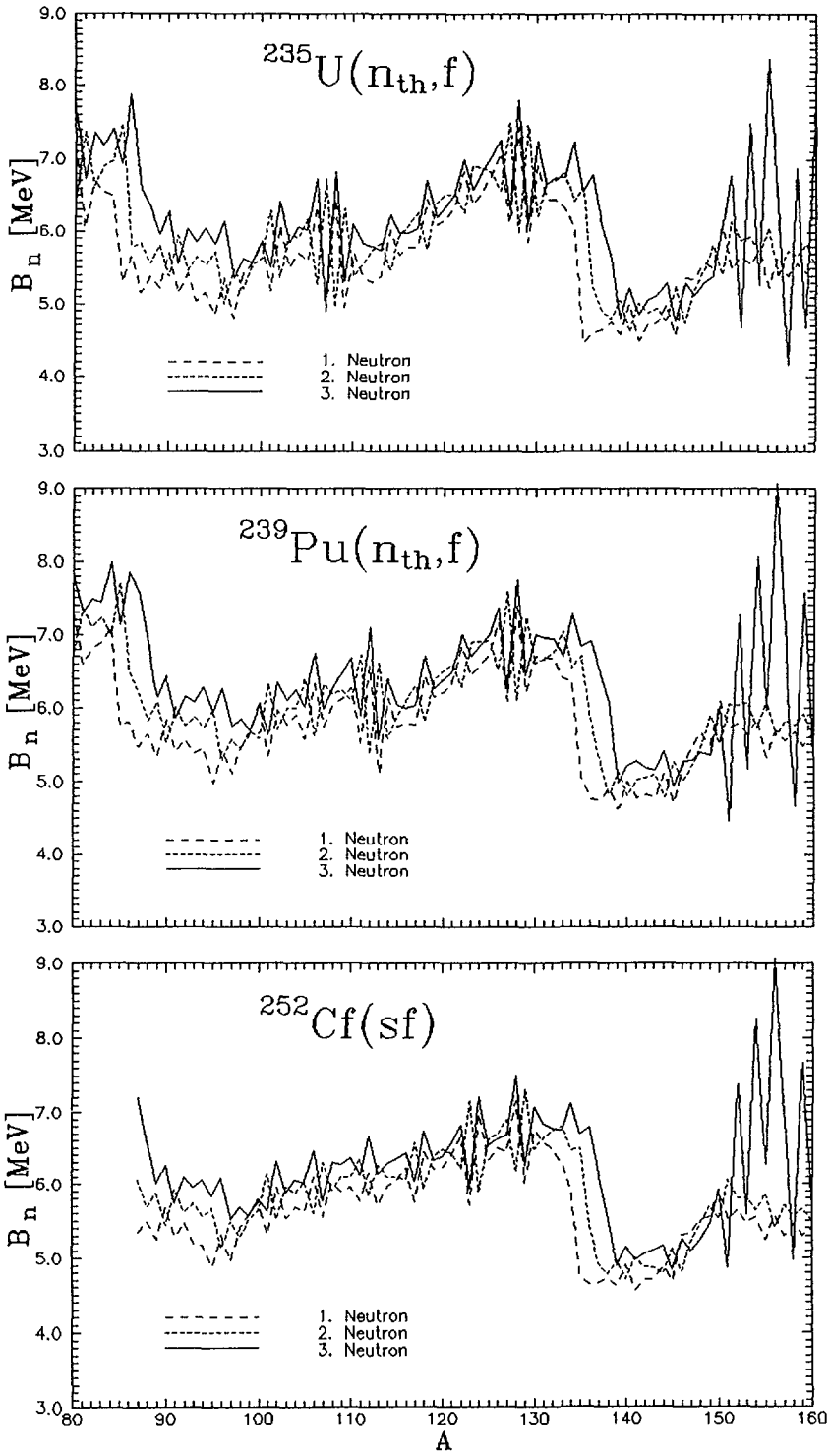

Fig. 5 Calculated neutron separation energy for fission fragments as function of mass number for the neutron induced fission of ^{235}U and ^{239}Pu and for the spontaneous fission of ^{252}Cf. The solid, short dashed, and long dashed lines correspond to the emission of the first, the second, and the third neutron, respectively.

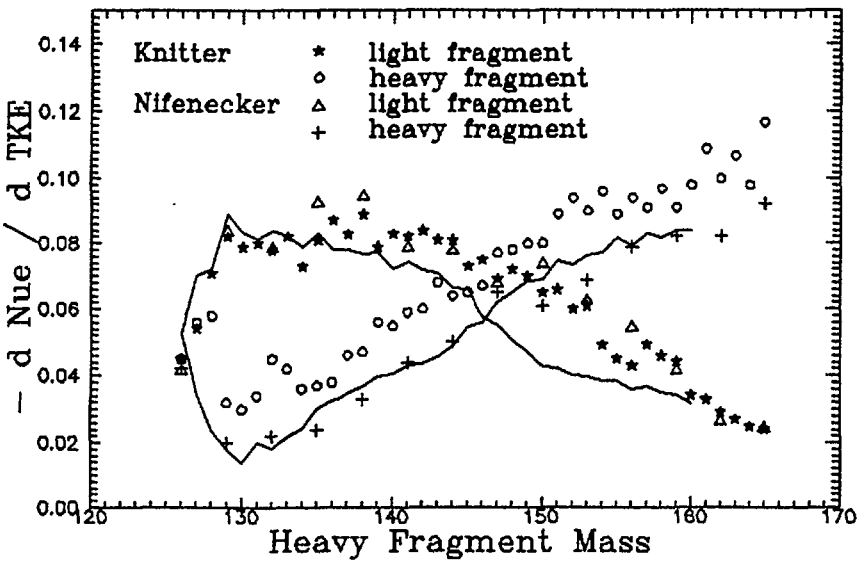

Fig. 6 Calculated slope $[\partial\bar{\nu}/\partial TKE](A)$ for $^{252}Cf(sf)$ in comparison with experimental data /18,20/

experimental results. Thus, the conclusion can be drawn that the variation of $\bar{\nu}$ as function of TKE for the fragments of a given mass split can be understood as an effect of the fragment stiffness at scission influenced by the shell structure. The linearity in this behavior points to a nearly constant stiffness of the individual fragments.

5. MULTIPLE-CHANCE FISSION

In the case of higher incidence energies the emission of one ore more neutrons prior to fission becomes energetically possible. To account for this multiple chance fission, in general (n,jnf), the neutron multiplicities $\bar{\nu}_j(E_i)$ have been separately calculated for each chance j considering the diminution of compound nucleus excitation. The weight of each chance is identical with partial fission cross section $\sigma_{f,j}(E_i)$ to be calculated within reaction theory including the fission channel. Consequently, the total neutron multiplicity (pre-fission neutrons together with post-fission neutrons) is given by

$$\bar{\nu}_{tot}(E_i) = \frac{1}{\sigma_{f,tot}} \sum_{j=0}^{j_{max}} (\bar{\nu}_j(E_i) + j) \sigma_{f,j}(E_i) \qquad (11)$$

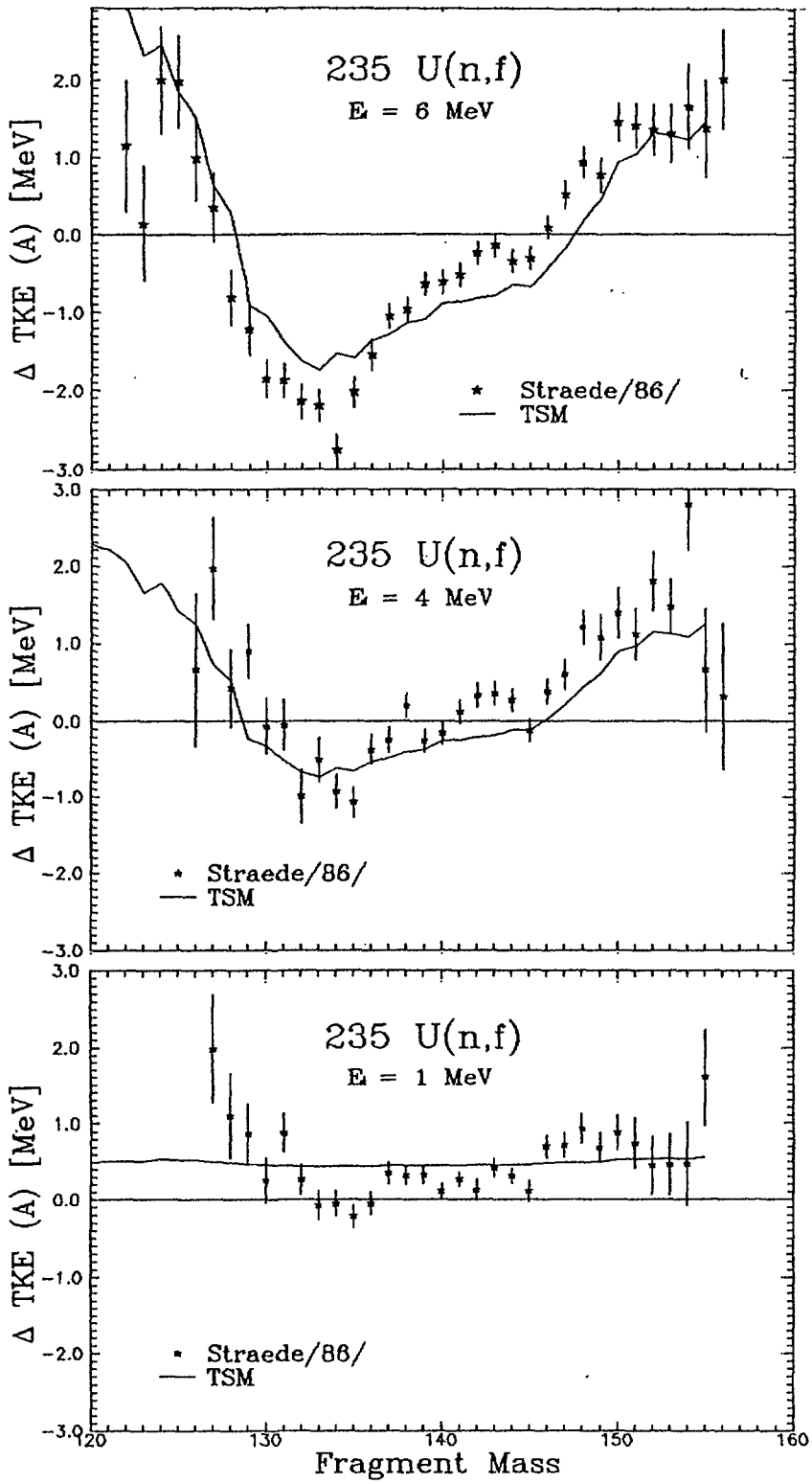

Fig. 7 Total kinetic energy of complementary fission fragments from ^{235}U(n,f) for 3 different incidence energies shown as difference to the value for thermal neutron induced fission (line - TSM, points - Straede /7/)

6. NEUTRON MULTIPLICITY IN INDUCED FISSION

A remarkable test of the accuracy of description of energy partition and neutron emission within the TSM was the study of several trends in TKE depending on fragment mass split and excitation energy of the fission nucleus. Therefore, these results /1/ are included before discussing the calculated neutron multiplicities. In general, an increasing incidence energy gives rise to a diminution of shell effects due to the higher excitation at scission. As presented in Fig. 7 for the neutron induced fission of ^{235}U, this is connected with a decrease of TKE in the TKE-maximum region (heavy fragments with A $\approx$ 130) and with an increase in the symmetric and strong asymmetric mass split region. However, there are deviations from this general behavior which differ for various fission reactions in the case of small incidence energies. In the framework of the TSM these changes in TKE can be explained by alterations in the heat energy above the second fission barrier due to pair breaking /1/. For E^*_{cn} within the pairing gap above the second saddle point, an increasing incidence energy give rise to higher TKE of the fission fragments. This circumstance is, however, effected by the second barrier height with reference to the first one. Whereas $E_{f,A}$ is lower than $E_{f,B}$ in the sub-U region (cf. example in Fig.8), the opposite behaviour was observed for actinides heavier than U. In the first case, pairing effects at saddle B are essential. A consequence is the characteristic dependence of TKE on incidence energy for Th, U, and Pu as shown in Fig. 9.

For this investigation as well as for the calculation of average neutron multiplicities, the knowledge of the fragment mass distribution Y(A) is required. It is approximated by a 5-Gaussian approach representing two asymmetric and one symmetric fission mode. The set of Gaussian parameters (including account for multiple-chance fission) was obtained by a complex fit as function of mass number of compound nucleus and incidence energy in the Th - Cf region. In Fig. 10, this approximation is shown for the thermal neutron induced fission of ^{235}U according to Straede /7/.

Finally, calculated average neutron multiplicities are shown for several fission reaction up to 20 MeV incidence energy. As described in paragraph 5, one has to account for multiple-chance

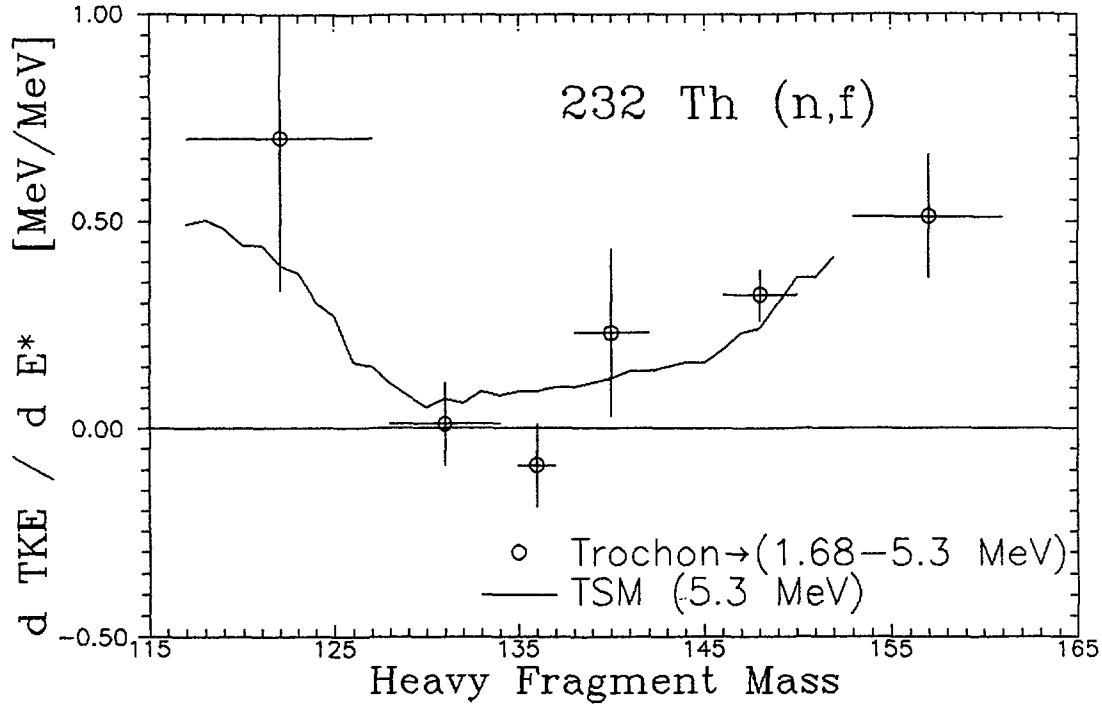

Fig. 8 Total kinetic energy as difference to the value of threshold fission plotted as function of the heavy fragment mass (solid line - TSM, points - Trochon /22/)

fission in this case. In the Figs. 11 - 13, average neutron multiplicities (including pre-fission neutrons!) as function of incidence energy are presented. The experimental data /26-28/ are well reproduced by TSM calculations.

Fig.11 shows $\bar{\nu}(E_i)$ for the neutron induced fission of ^{232}Th. In contrast to other fission nuclei (Fig. 12 and 13), there is a remarkable step-like behavior in $\bar{\nu}(E_i)$ above the threshold of the second chance ($\cong$ 6 MeV). Considering the higher neutron multiplicity of this chance $\bar{\nu}_2$ (enhanced by the post-fission neutron) this is due to the relative high values of the partial fission cross section for the second chance.

7. SUMMARY

It was shown that the calculation of fission neutron multiplicities requires a model for solving the energy partition problem in nuclear fission. The TSM as an energy-conservation consistent scission point model with semi-empirical, temperature-dependent shell correction energies for deformed fragments at scission is successful in describing the main fission

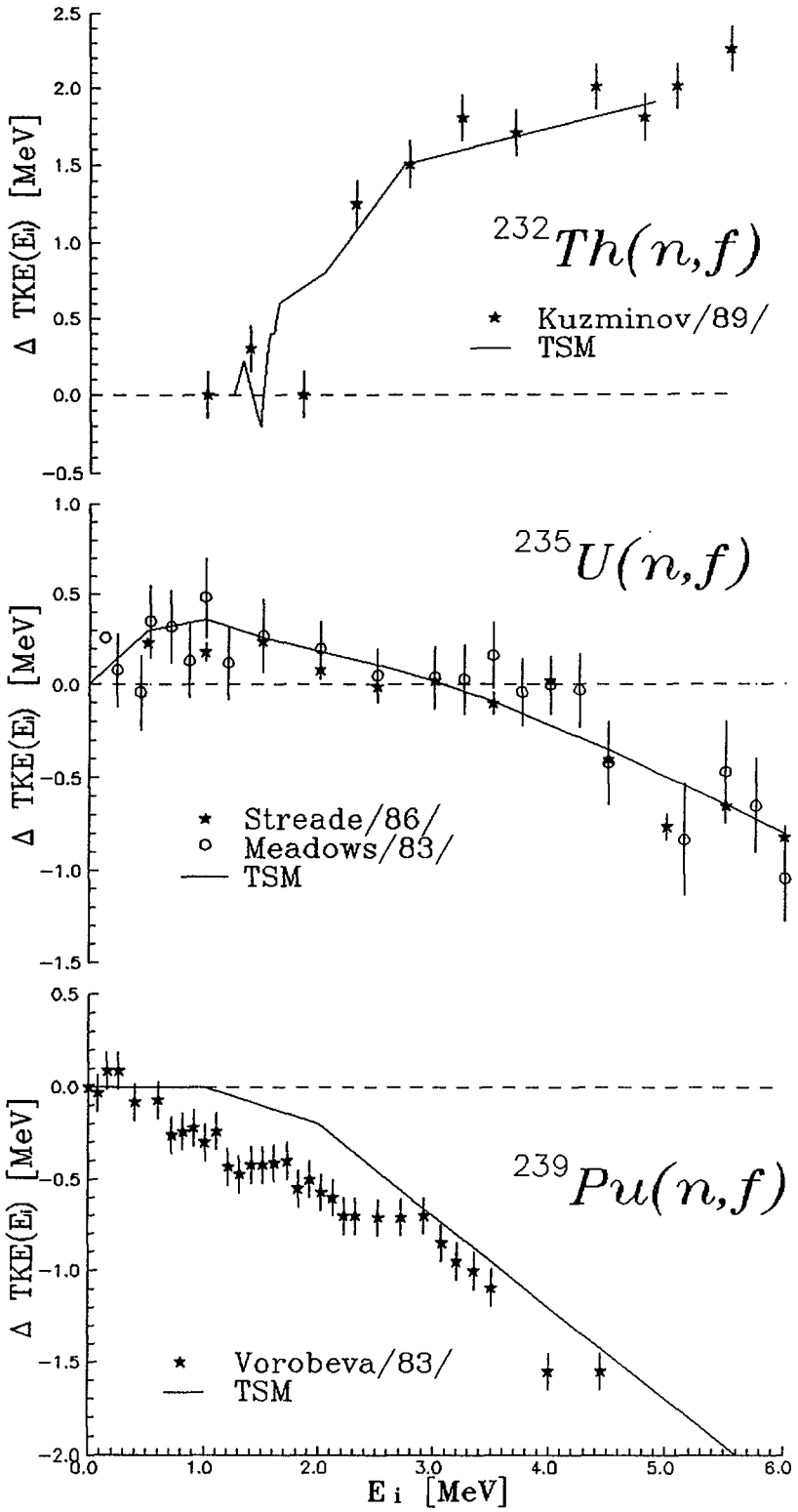

Fig. 9 Calculated average $\overline{TKE}$ as difference to the value of minimum (thermal or threshold) incidence energy for different incidence energies and various fissioning nuclei in comparison with experimental data /7/, /23-25/.

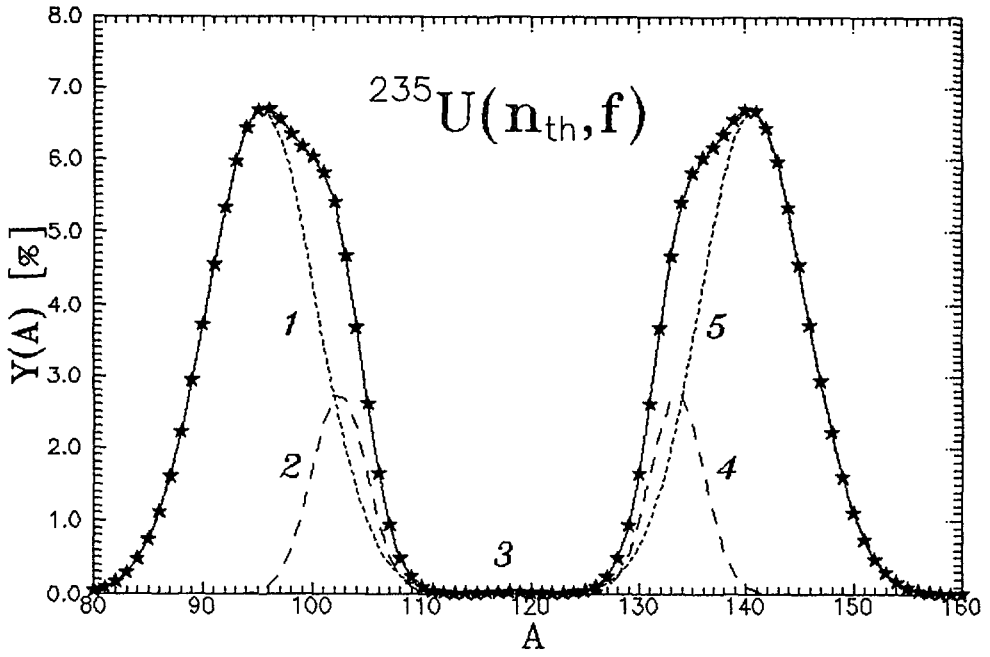

Fig. 10 5-Gaussian approximation of fragment mass yield distribution for $^{235}U(n_{th},f)$ according to Straede [7]

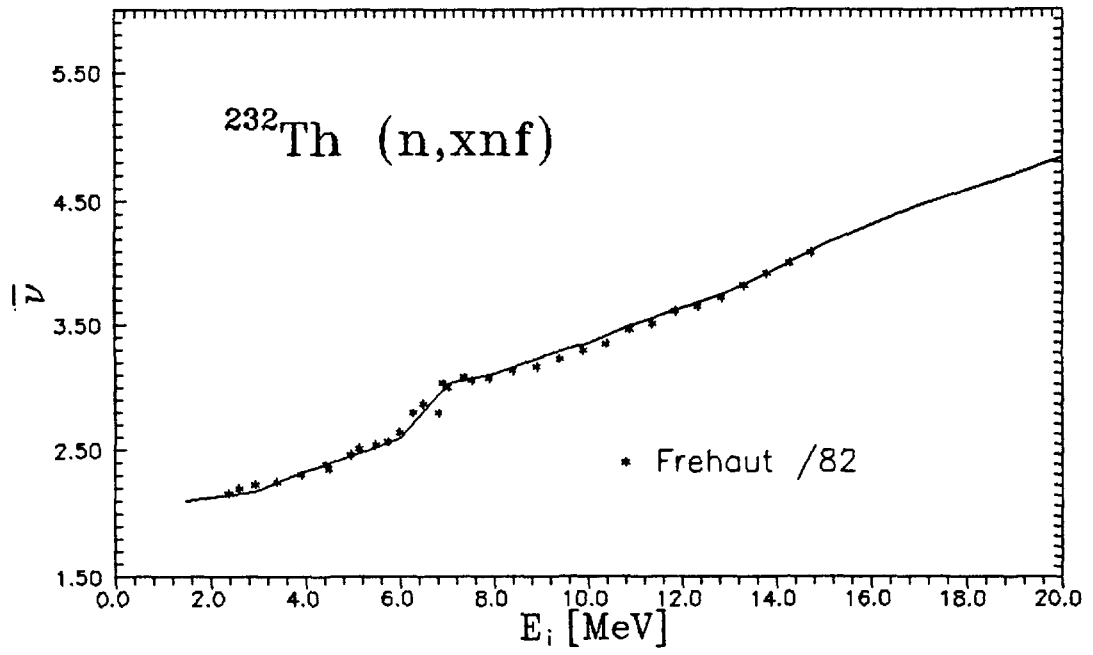

Fig. 11 Average neutron multiplicity as function of incidence energy for the neutron induced fission of ^{232}Th (experimental data were taken from Ref. /26/)

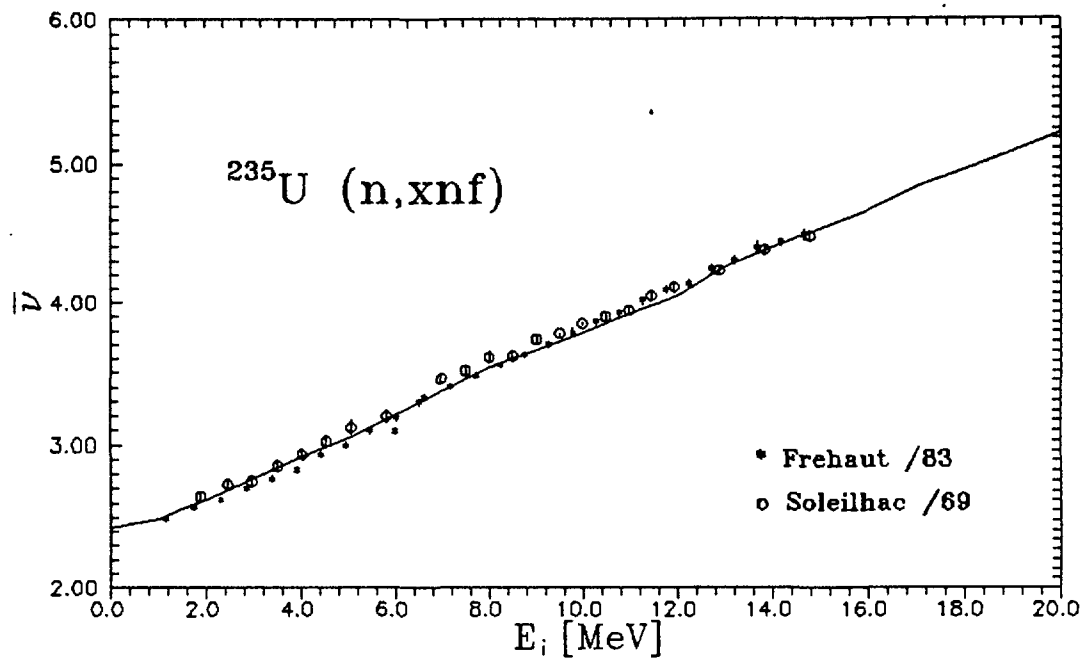

Fig. 12 Average neutron multiplicity as function of incidence energy for ^{235}U(n,f) (experimental data were taken from Ref. /26-27/)

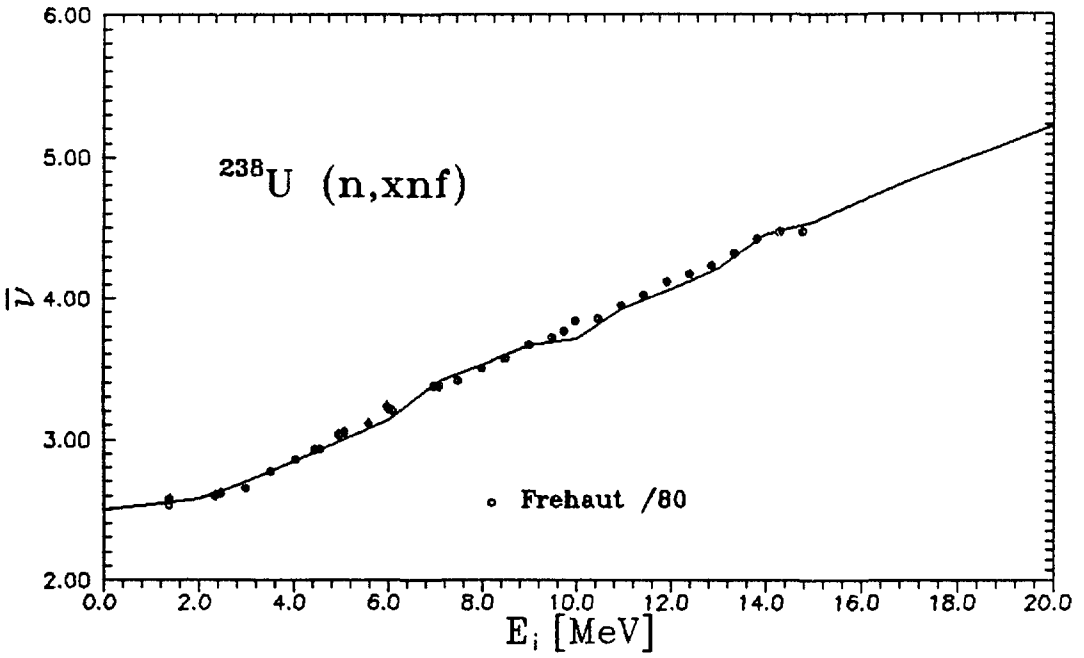

Fig. 13 Average neutron multiplicity as function of incidence energy for ^{238}U(n,f) (experimental data were taken from Ref. /28/)

fragment characteristics. As a test of the accuracy of the TSM calculations several trends in TKE data for induced fission were discussed. The average fragment excitation energies were used to obtain neutron multiplicities by the help of an energy balance of fragment de-excitation, which includes neutron evaporation and γ-ray emission. As shown by several examples, the dependence of $\bar{\nu}$ on incidence energy is well reproduced by the TSM. The TSM provides the basis for several applications as the calculation of fragment data as well as neutron emission probabilities. It is an essential basis for a fission neutron data systematics.

References

/ 1/ A.Ruben, H. Märten, and D. Seeliger, Z. Phys. **A 338**, 67 (1991)
/ 2/ J. Kristiak and J. Kliman, Proc. 5th Int. Symp. on Neutron Induced Reactions, Smolenice, 1988, Physics and Applications, Vol. **15**, ed. S. Gmuca, R. Antalik, and J. Kristiak, p. 305 (1988)
/ 3/ J. Terrell, Proc. IAEA Symp. on Phys. and Chem. of Fission, Salzburg, 1965 (Vienna, 1965) Vol. II, p. 3
/ 4/ M. Kildir and N.K. Aras, Phys. Rev. **C25**, 365 (1982)
/ 5/ A. V. Ignatjuk et al., Yad. Fiz. **42**, 569 (1985)
/ 6/ W. F. Apalin et al., Nucl. Phys. **71**, 553 (1965)
/ 7/ C. A. Straede et al., Nucl. Phys. **A462**, 85 (1987)
/ 8/ F. Gönnenwein et al., Proc. XVIIth Int. Symp. on Nucl. Phys., Gaussig (GDR), 1987, ZfK-**646**, 129 (1988)
/ 9/ R. J. Lipinski and B. W. Wehring, Phys.Lett. **66B**, 326 (1977)
/10/ W. Lang, PhD Thesis, "Nuklidausbeuten bei der Reaktion 235-U(n,f) als Funktion der kinetischen Energie der Spaltprodukte - Ein experimenteller Zugang zur Dynamik des Spaltprozesses", TH Darmstadt (1979)
/11/ S. Amiel et al., Phys. Rev. **C15**, 2119 (1977)
/12/ T. Izak-Biran and S. Amiel, Phys. Rev. **96**, 1059 (1954)
/13/ W. W. Malinovski, Yad. Const. **2**, 25 (1987)
/14/ J. P. Unik et al, Proc. IAEA Symp. on Phys. and Chem. of Fission, Rochester 1973, IAEA Vienna 1974, Vol II, p.19
/15/ Y. Ando et al., Report **JAERI-M83-025** (1983)
/16/ A. C. Wahl, Atomic Data and Nuclear Data Tables **39**, 1 (1988)
/17/ J. Frehaut, Proc. of Cons. Meeting on Physics of Neutron Emission in Fission, Mito, 1988 (IAEA Wien, 1989) INDC(NDS)-**220**, 99
/18/ H. Nifenecker et al., Proc. IAEA Symp. on the Physics and Chemistry of Fission, Rochester, 1973 (IAEA, Vienna, 1974), Vol. II, p.117
/19/ R. Schmidt-Fabian, PhD Thesis, "Messung der spontanen Spaltung von 252-Cf am Darmstadt-Heidelberger Kristallkugel-Spektrometer", Ruprecht-Karls-Universitat Heidelberg (1988)
/20/ C. Budtz-Jorgenson and H.-H. Knitter, Nucl. Phys. **A490**, 307 (1988)
/21/ A. Ruben, and H. Märten, Z. Phys **A 337**, 237 (1990)
/22/ J. Trochon et al., Nucl. Phys. **A318**, 63 (1979)

/23/ A. A. Goveerdovski, B. D. Kuzminov, V. F. Mitranov, and A. I. Sergachev, Proc. of Cons. Meeting on Physics of neutron emission in fission, Mito 1988, IAEA, INDC(NDS)-220, p.59
/24/ V. G. Vorob'eva, B. D. Kuz'minov, and V. N. Manokhin, Report IAEA, INDC(CCP)-128/G+Sp
/25/ J. W. Meadows, Phys. Rev. **177**, 1817 (1969)
/26/ J. Frehaut et al., Proc. of Intern. Conf. on Nucl. Data for Science and Technology, 6-10 Sept. 1982, Antwerp D. Reidel Publishing Company, p. 78 (1983)
/27/ M. Soleilhac et al., Nucl. Energy **23**, 257 (1969)
/28/ J. Frehaut et al., "Recent results on $\bar{\nu}$-prompt measurements between 1.5 and 15 MeV", Paris (1980)